Supplementary Information (SI) for Dalton Transactions.
This journal is © The Royal Society of Chemistry 2025

Gold bis(dithiolene) radical turning metallic under pressure: fusing pyrazine and dithiine rings on a dithiolene ligand

Haia Kharraz,[a] Pere Alemany,[b] Enric Canadell,*[c,d] Thierry Roisnel,[a] Hengbo Cui,[e] Kee Hoon Kim,[e] Marc Fourmigué*[a] and Dominique Lorcy*[a]

Supplementary Information

Synthesis and properties of $[Et_4N][Ni(pzdtdt)_2]$ p 1

Figures S1 – S5 p 1

Tables S1 – S2 p 6

Synthesis and properties of [Et_4N][Ni(pzdtdt)$_2$]

Synthesis. Under an inert atmosphere, a solution of MeONa (Na: 0.12 g, 5.4 mmol) in MeOH (6 mL) was added to **2** (0.15 g, 0.54 mmol) and heated up for 1h. After complete dissolution, the solution was stirred for 30 min at room temperature. Then a solution of $NiCl_2.6H_2O$ (0.06 g, 0.27 mmol) in MeOH (5 mL) was added, followed 6 hours later by the addition of Et_4NBr (0.17 g, 0.54 mmol). After stirring for 15 h, the formed precipitate was filtered and recrystallized from acetonitrile to afford the monoanionic complex [Et_4N][Ni(pzdtdt)$_2$] as black crystals with an 34% yield. MP = 240°C Anal. Calcd for $C_{20}H_{24}N_5NiS_8$ + MeOH: C, 37.00; H, 4.14; N, 10.27. Found: C, 36.90; H, 4.58; N, 10.37.

Electrochemistry. Cyclic voltammetry of [Et_4N][Ni(pzdtdt)$_2$] (Fig. S1), performed in CH_3CN with Bu_4NPF_6 0.1 M as an electrolyte at a scan rate of 100 mV/s with SCE reference, shows a reversible reduction wave associated to the −2/−1 redox process at −0.36 V *vs*. SCE, and an irreversible oxidation associated to the −1/0 redox process with anodic and cathodic peak potentials at +0.29 and +0.04 V *vs*. SCE respectively.

Crystallography. Details about X-ray data collection and refinement are found in Table S1. Molecular structure and solid-state arrangement are shown in Figs. S3 and S4. Bond distances and angles are given in Table S2. The shape of this complex presents some similarities with that of the monoanionic gold complex in [Ph_4P][Au(pzdtdt)$_2$], which is to say a 1,4-dithiine ring folded around the S---S hinge with a dihedral angle between the planes of 49.5(2)° and a slightly folded NiS_2C_2 metallacycle along the S---S hinge by 4.8°).

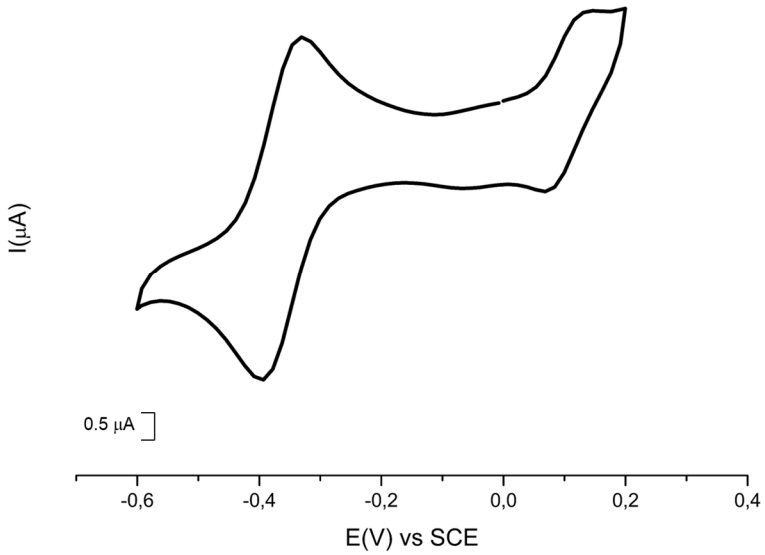

Fig. S1 Cyclic voltammetry of $[Et_4N][Ni(pzdtdt)_2]$, performed in CH_3CN with Bu_4NPF_6 0.1 M as electrolyte at a scan rate of 100 mV/s, with SCE reference.

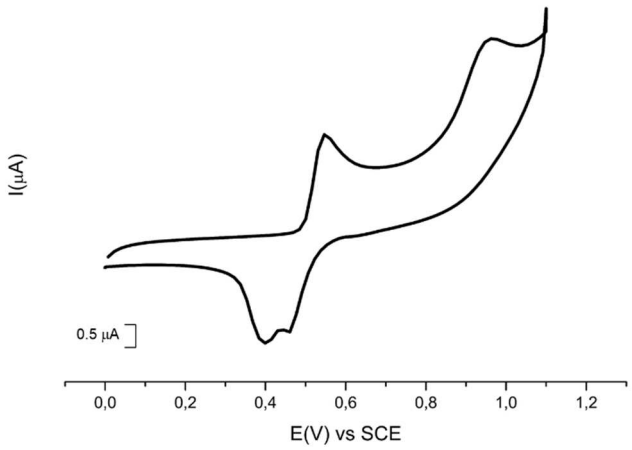

Fig. S2 Cyclic voltammetry of $[Ph_4P][Au(pzdtdt)_2]$, performed in CH_3CN with Bu_4NPF_6 0.1 M as electrolyte at a scan rate of 100 mV/s, with SCE reference.

(a)

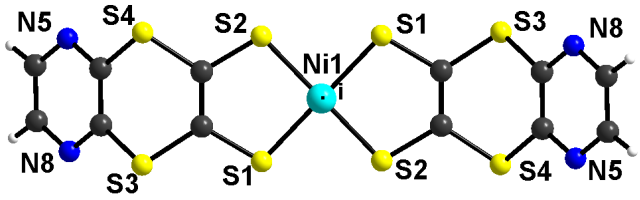

(b)

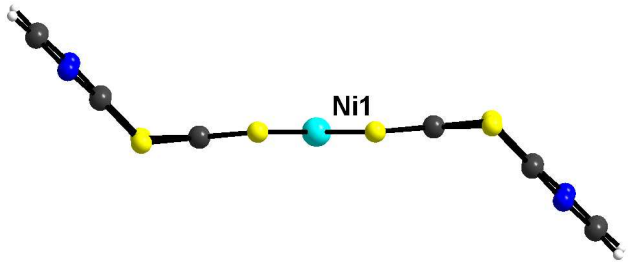

Fig. S3 Molecular structure of $[Ni(pzdtdt)_2]^-$ in $[Et_4N][Ni(pzdtdt)_2]$.

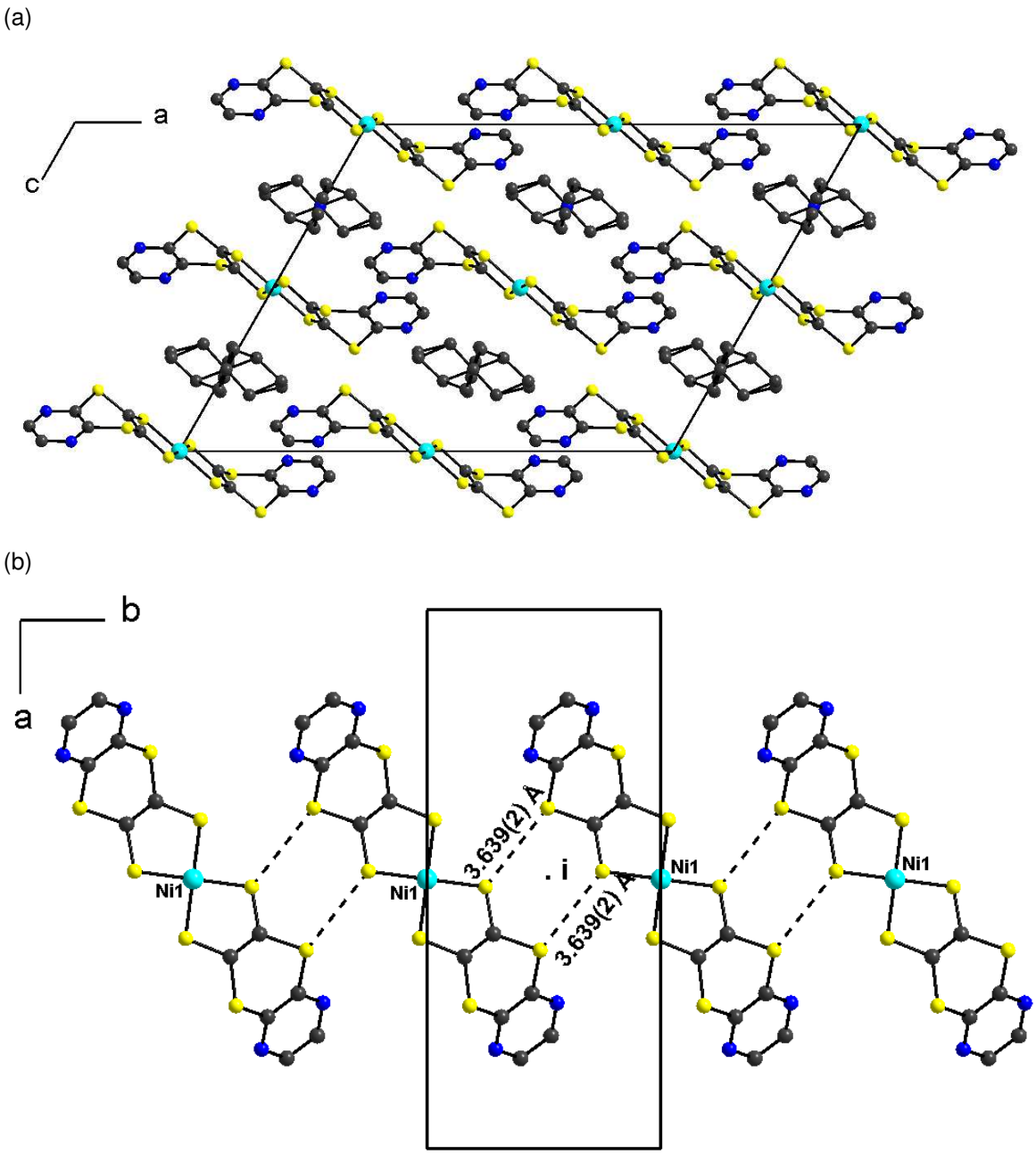

Fig. S4 Solid state arrangement of $[Et_4N][Ni(pzdtdt)_2]$ with (a) projection view along *b* of the unit cell and, (b) detail of the chain of $[Ni(pzdtdt)_2]$– radical anions running along *b* with weak lateral S•••S intermolecular interactions. The shortest S•••S distance at 3.639(2) Å exceeds the S•••S van der Waals contact distance of 3.60 Å.

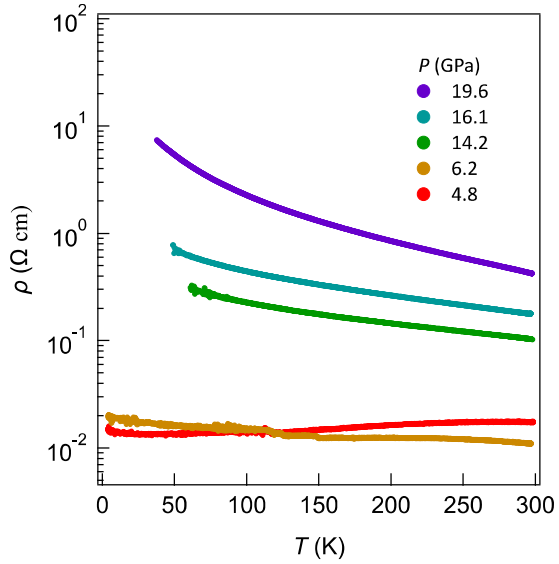

Fig. S5 Temperature dependence of the resistivity of $[Au(pzdtdt)_2]^{\bullet}$ at different applied pressures

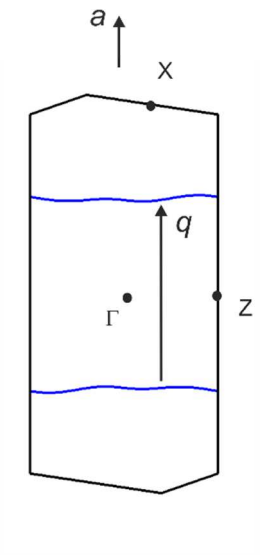

Fig. S6 Calculated Fermi surface associated with the band structure shown in Fig. 2.

Table S1 Crystallographic data[a,b]

	1	**2**	$[Et_4N][Ni(pzdtdt)_2]$	$[Ph_4P][Au(pzdtdt)_2]$	$[Au(pzdtdt)_2]^{\bullet}$
CCDC	2422633	2422634	2422635	2422637	2422636
Formulae	$C_7H_2N_2S_5$	$C_7H_2N_2S_5$	$C_{20}H_{24}N_5NiS_8$	$C_{36}H_{24}AuN_4PS_8$	$C_{12}H_4AuN_4S_8$
FW ($g.mol^{-1}$)	274.41	258.35	649.63	997.01	657.64
System	orthorhombic	monoclinic	monoclinic	triclinic	monoclinic
Space group	Pnma	$P2_1/n$	C2/c	P-1	$P2_1/n$
a (Å)	23.107(3)	12.5503(10)	21.976(2)	8.4285(8)	3.7034(5)
b (Å)	10.6201(13)	3.8827(3)	8.3085(8)	11.7655(11)	30.203(4)
c (Å)	3.9168(5)	19.3569(17)	16.7017(17)	19.481(2)	7.5483(9)
α (deg)	90.00	90.00	90.00	104.095(4)	90.00
β (deg)	90.00	101.122(3)	119.994(3)	99.229(4)	98.492(5)
γ (deg)	90.00	90.00	90.00	90.809(4)	90.00
V ($Å^3$)	961.2(2)	925.53(13)	2641.1(4)	1846.6(3)	835.05(18)
T (K)	150(2)	150(2)	150(2)	150(2)	150(2)
Z	4	4	4	2	2
Cryst. dim. (mm)	0.41×0.03×0.02	0.49×0.14×0.07	0.23×0.17×0.10	0.36×0.21×0.05	0.29×0.04×0.025
D_{calc} ($g.cm^{-3}$)	1.896	1.854	1.634	1.793	2.615
μ (mm^{-1})	1.157	0.986	1.389	4.514	9.814
Absorption corr.	multi-scan	multi-scan	multi-scan	multi-scan	multi-scan
T_{min}, T_{max}	0.632, 0.977	0.778, 0.933	0.784, 0.870	0.573, 0.798	0.571, 0.782
Total refls	9822	9875	15252	21288	7629
Uniq refls (R_{int})	1175 (0.0638)	2056 (0.0235)	3026(0.0262)	8370 (0.0284)	1914 (0.0308)
Uniq refls (I > 2σ(I))	1082	1996	2822	7390	1848
R_1, wR_2	0.0390, 0.0770	0.0214, 0.0582	0.0245, 0.0658	0.0263, 0.0715	0.0477, 0.1100
R_1, wR_2 (all data)	0.0420, 0.0784	0.0221,	0.0264, 0.0674	0.0310, 0.0755	0.0497, 0.1106
GOF	1.162	1.057	1.042	0.987	1.534

[a] $R_1 = ||F_o| - |F_c||/|F_o|$. [b] $wR_2 = [w(F_o^2 - F_c^2)^2]/[w(F_{o2})^2]^{1/2}$.

Table S2 Bond lengths (in Å) and dihedral angles (in °) in the monoanionic $[Ni(pzdtdt)_2]^{-1}$ complex and analogous complexes.

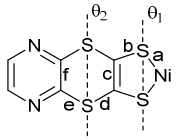

pzdtdt ligand

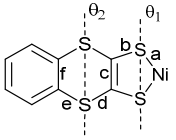

bdtdt ligand

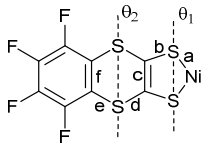

F_4bdtdt ligand

Complex		a	b	c	d	e	f	θ_1	θ_2	Ref
$[Ni(pzdtdt)_2]^{-1}$		2.1583(4)	1.7300(16)	1.356(2)	1.7673(15)	1.7707(16)	1.404(2)	4.8(6)	49.5(2)	this work
		2.1497(4)	1.7256(15)		1.7675(16)	1.7611(15)				
$[Ni(bdtdt)_2]^{-1}$		2.147(1)	1.726(4)	1.351(5)	1.757(5)	1.758(4)	1.399(6)	6.7(5)	48.0(7)	1
		2.144(1)	1.728(5)		1.754(4)	1.767(4)				
$[Ni(F_4bdtdt)_2]^{-1}$	*Mol 1*	2.149(1)	1.721(3)	1.347(4)	1.760(3)	1.760(3)	1.391(3)	3.98(5)	50.6(1)	1
		2.158(2)	1.732(3)		1.761(3)	1.767(3)				
	Mol 2	2.159(1)	1.730(3)	1.349(4)	1.763(2)	1.761(3)	1.398(4)	7.0(3)	47.8(4)	
		2.151(1)	1.724(3)		1.764(3)	1.763(3)				

[1] Q. Yu, J.-Y. Ge, Z.-P. Lv, H.-Y. Wang and J.-L. Zuo, Structure-dependent electronic transition in a new type of π-electron delocalized multi-sulfur bis(dithiolene)nickel complex, *RSC Adv*., 2016, **6**, 100783–100789.